Mechanical behaviour of an artificially microcracked marble
Comportement mécanique d'un marbre microfissuré artificiellement
Mechanisches Verhalten von einem künstlich Haargerissenen marmor

T. Rotonda
Dip. Ing. Strutt. e Geotecnica, University "La Sapienza", Rome, Italy

ABSTRACT: To investigate the influence of microcracking conditions on the mechanical bahaviour of rocks, a homogeneous isotropic rock (Carrara marble) was slowly heated at temperatures from 50 to 300°C. On these specimens tests were carried out to determine strength, deformability and dynamic properties in uniaxial and triaxial conditions. Static deformability and dynamic properties are markedly reduced by even only mild microcracking, whereas strength is less influenced. The effect of microcracking is felt more in tensile conditions and less in uniaxial compression conditions. The influence of saturation and of the applied load on the compressional and shear wave velocities is also discussed and the results are compared with some theoretical models of microcracked media.

RESUME: Pour étudier l'influence de la microfissuration sur les roches, une roche isotrope homogène (marbre de Carrara) a été chauffée lentement avec températures de 50 a 300°C. On a fait des essais sur ces échantillons pour en déterminer la résistance, la déformabilité et les propriétés dynamiques en conditions uniaxiales et triaxiales. La déformabilité statique et les propriétés dynamiques diminuent par effet des microfissures, même légères, tandis que la résistance est moins influencée. L'effet de la microfissuration est plus fort dans les conditions de traction et moins fort dans les conditions de compression uniaxiale. On a examiné aussi l'influence de la saturation et de la charge appliquée sur les vélocités d'onde de compression et de cisaillement; les résultats sont comparés avec des modèles théoriques de moyens microfissurés.

ZUSAMMENFASSUNG: Um den Einfluss von Haarrissen auf das mechanische Verhalten der Felsen zu prüfen, wurde ein homogenes isotropes Fels (carrarischer Marmor) langsam von 50°C bis 300°C aufgeheizt. Die Untersuchungen wurden weitergeführt, um Festigkeit, Verformbarkeit und dynamische Eigenschaften der Proben in ein-und dreiachsigen Zuständen zu bestimmen. Auch der geringste Haarriss kann sowohl die statische Verformbarkeit als auch die dynamischen Besonderheiten stark beschränken; er wirkt aber in einem geringeren Mass auf die Festigkeit ein. Eine solche wirkung zeigte sich deutlicher in Zugzustand als in einachsigem Kompressionszustand. Untersucht wurde auch die Einwirkung, die Sättigung und aufgebrachte Belastung auf die Kompressions-und Scherwellegeschwindikeiten haben.

1 INTRODUCTION

Pervasive microcracking is present in most hard brittle rocks and its influence on their mechanical and transport properties has been studied extensively for many years now. Growth of microcracks in near-surface rocks is usually attributed to internal stresses at grain level produced by changes in temperature and in macroscopic stresses during uplift (Nur & Simmons, 1970; Bruner, 1984). However, microcracks can in some cases also be ascribed to the effect of active tectonic stresses.

In recent years studies for radioactive waste disposal and for the exploitation of geothermal energy have focused researchers' attention on the thermal behaviour of rocks, on the modification of microcracking patterns caused by slow heating and on the ensuing influence on their thermomechanical behaviour (Simmons & Cooper, 1978; Bauer & Johnson, 1979; Bauer & Handin, 1983; Homand-Etienne & Houpert, 1989).

Thermal microcracking in controlled conditions can also be generated in a rock with the aim to produce a homogeneous model material with a varying, well defined, intensity of microcracks. Tests on this material are useful to validate "damage" theories (Kawamoto et al., 1988) on rock behaviour and to study the influence of applied stresses and of saturation conditions on the mechanical and transport properties of the rocks; even the behaviour of some types of rock masses, which are composed of tightly interlocked blocks, can be simulated in this way (Rosengren & Jaeger, 1968; Gerogiannopoulos & Brown, 1978).

For this reason it was deemed useful to investigate the characteristics of an artificially cracked material obtained from a very homogeneous and isotropic rock with negligible initial microcrack density. The tested rock is a white Carrara marble consisting of calcite crystals with a grain size of about 0.2-0.3 mm and negligible amounts of other minerals.

2 CHARACTERISTICS OT THE TESTED ROCK

The main characteristics of the rock were determined on cylindrical specimens (54mm in diameter) cored from a single high quality block. Porosity (ϕ), compressional and shear wave velocities (V_P and V_S), uniaxial compressive strength (σ_f) and Young modulus (E) were determined on specimens having a height to diameter ratio of 2. The axial and transversal strains were determined with 2 vertical and 2 horizontal strain gauges (10 mm in length); a strain rate of

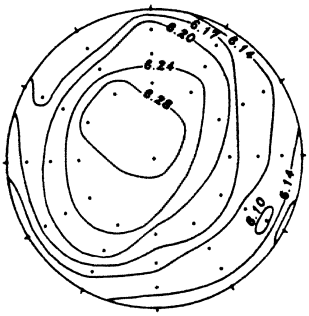

Figure 1. Compressional wave velocity as a function of direction determined on a spherical specimen of Carrara marble (equal area projection)

$4 \cdot 10^{-6}$ s^{-1} was adopted. Brazil tests to determine the indirect tensile strength (σ_t) were carried out on specimens whose thickness was half their diameter.

The experimental results are summarized in table 1. The low values of the variation coefficients (V) confirm the high homogeneity of the tested specimens; this obviously facilitates the observation of the effects of even slight variations in microcrack intensity.

Total porosity, shown in table 1, was determined from the values of the density of regular specimens (obtained from accurate dimensional measures) and from grain density. The porosity determined on the basis of water content in saturated conditions is only about $1 \cdot 10^{-3}$, which means that most pores are isolated; some isometric pores, about 0.5 mm in size, were in fact observed in the rock during the preparation of the specimens.

Table 1. Principal characteristics of the Carrara marble

	ϕ ($\cdot 10^{-3}$)	V_P (km/s)	V_S (km/s)	σ_f (MPa)	σ_t (MPa)	E (GPa)
< >	3.83	6.26	3.09	98.2	10.2	77.6
s	0.27	0.09	0.04	3.0	0.5	1.5
V(%)	7.1	1.5	1.3	3.1	4.6	1.9
N	49	50	50	4	10	4

< >, average value;
s, standard deviation of the sample;
V, variation coefficient; N, number of tests

Because a slight chromatic banding ("macchia") and the metamorphic origin of the rock could suggest the presence of a weak oriented texture, P-wave velocities were measured in 36 directions utilizing a spherical specimen (110 mm in diameter), according to the technique proposed by Thill et al. (1968). The results (fig.1) actually indicate a polar symmetry but the degree of anisotropy is very small (about 2%).

The seismic velocities and the elastic properties of the marble, even at low stress values, are only slightly different from the theoretical values of a calcite aggregate calculated by the VRH averaging technique (Simmons & Wang, 1971) (although some discrepancies are found in the values given by various researchers); this confirms that the porosity of the rock is mostly due to pores having a high aspect ratio and that microcracking is negligible.

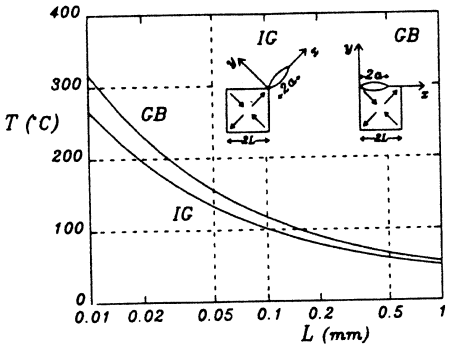

Figure 2. Threshold temperatures for the propagation of intergranular (IG) and grain boundary cracks (GB) in a calcitic rock as a function of grain dimension. The ratio between the length of the initial flaw and the grain dimension is assumed to be 0.05 and the critical stress intensity factor 0.2 MPa $m^{1/2}$

3 THERMAL CRACKING

Microcracking was produced by slowly heating the specimens in an oven, at a rate of 30°C/h, to predetermined temperatures (50, 100, 200 and 300°C); the maximum temperature was maintained for 4 hours and for the subsequent cooling the same rate of 30°C/h was adopted. The difference in temperature between the centre and the boundary of the specimen was less than 1°C as a result of this heating and cooling pattern, and thus the stresses caused by the thermal gradient were negligible.

In these conditions the thermal cracking of a monomineralic rock, as is the marble, is caused by the internal stresses arising from the anisotropy of the thermal expansion coefficients α_i of the crystals. The calcite crystal has uniaxial symmetry with $\alpha_3 = 26.4 \cdot 10^{-6}$ C^{-1} along the symmetry axis and $\alpha_1 = \alpha_2 = -5.3 \cdot 10^{-6}$ C^{-1} in the perpendicular directions (Skinner, 1966); the thermal anisotropy is therefore very strong with respect to other common rock minerals.

Various mechanical models have been adopted to evaluate the internal stresses caused by temperature variations in an aggregate of thermally anisotropic grains (Nur & Simmons, 1970; Johnson et al., 1978; Evans & Clark, 1980). Microscopic examinations of thermally cracked rock have shown the importance of polygonal grain shapes and of grain junctions on crack growth. A simple model in which this factor is accounted for has been proposed by Fredrich and Wong (1986); a single anisotropic crystal in the form of a square inclusion is considered to be embedded in a homogenized matrix with averaged thermal and elastic properties. Application of fracture mechanics principles, assuming a given ratio between initial flaw dimension and grain dimension, gives the threshold temperature for the propagation of cracks (fig.2). The threshold temperature strongly depends on grain size, as was experimentally observed in many rock types (Perami, 1971; Homand-Etienne & Houpert, 1989). A very low threshold temperature (about 75°C) is predicted for the marble.

Permanent axial strains after the thermal cycle were determined with a precision of $5 \cdot 10^{-5}$ on the same cylindrical specimens prepared for the uniaxial tests; volumetric strain was assumed to be 3 times the axial strain. Fig.3 shows that crack porosity varies with the square of the maximum temperature of the thermal

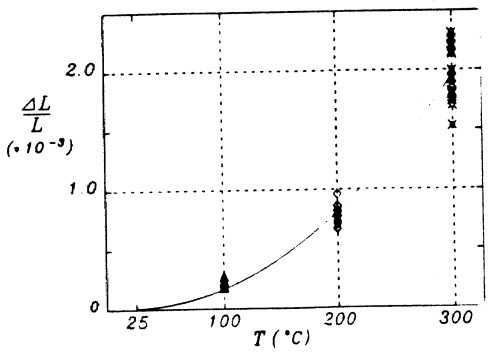

Figure 3. Permanent linear strains of marble specimens as a function of treatment temperature. The continuous curve was determined by means of a quadratic regression

cycle; it is to be noted that energy balance considerations (Fredrich & Wong, 1986) suggest a quadratic relation between the new crack surface per unit volume and the maximum temperature of the treatment. The porosity increase at 300°C is only $5 \cdot 10^{-3}$, a value only slightly larger than initial porosity.

Determination of water content at saturation for the thermally treated rock shows that most of the new crack porosity is interconnected (fig.4).

4 STRENGTH AND DEFORMABILITY OF THE CRACKED ROCK

The uniaxial compressive strength of thermally cracked specimens is plotted in fig.5 versus the crack porosity increase of each specimen. The Brazil tensile strength values are instead plotted in fig.5 as a function of the average crack porosity increase for each treatment temperature, because this increase was not determined in each of these specimens. The effect of cracking was found to be stronger on the tensile strength than on the compressive strength: for the 300°C specimens the former is reduced to 67% of the initial average value, the latter to 83%. The rate of strength decrease versus crack porosity is clearly greater at low porosity values; the effect of microcracking is already marked for the 100°C specimens, in which the crack porosity increase is less than $0.5 \cdot 10^{-3}$.

The shape of the stress-strain curves in uniaxial compression is very sensitive to microcracking: whereas the behaviour of the natural marble is almost linearly elastic up to 50% of the ultimate load

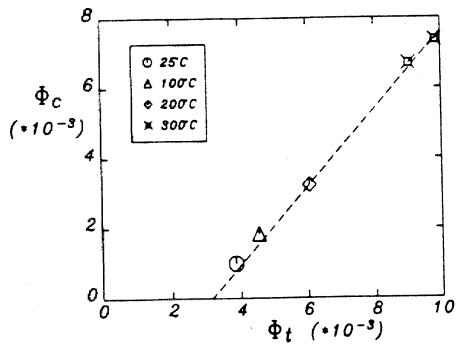

Figure 4. Comparison between total porosity ϕ_t (obtained from the dry specimen density and the grain density) and the connected porosity ϕ_c (obtained from water content at saturation)

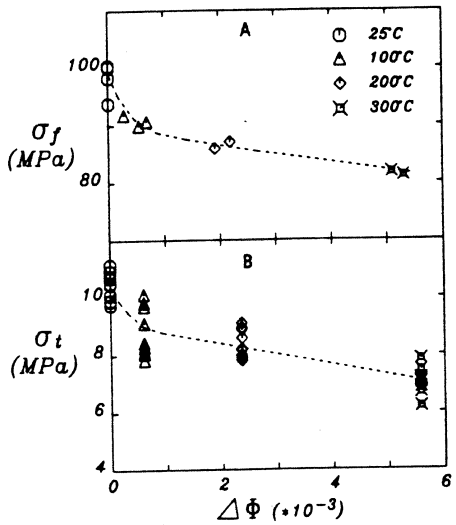

Figure 5. Uniaxial compressive strength as a function of crack porosity increase (A). Brazil tensile strength as a function of mean crack porosity increase for each temperature (B)

(fig.6), thermally treated specimens show an increase of the stiffness up to a stress level of about 40% of the ultimate load, followed by a gradual decrease up to failure (fig.7). However, the initial portion of the stress-strain curves of the thermally treated specimens shows a downward curvature up to 5-10 Mpa; the same behaviour is apparent in the volumetric strain curves. The transversal strain is only slightly affected by the microcracking, as predicted by theoretical models, so that the Poisson ratio decreases at increasing microcracking conditions.

Microcracking affects the stiffness of the rock more than the strength, so that in a Deere diagram the points representing the specimens treated at different temperatures are located along a steeply dipping curve, passing from the region of high modulus ratio to that of medium modulus ratio at increasing temperatures (fig.8).

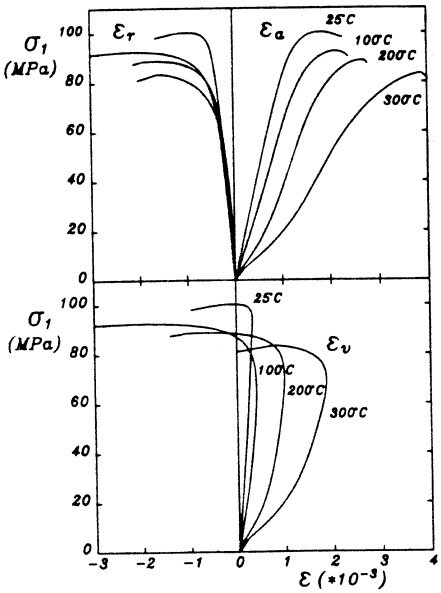

Figure 6. Axial, lateral and volumetric strain curves obtained in uniaxial compression tests on thermally treated specimens

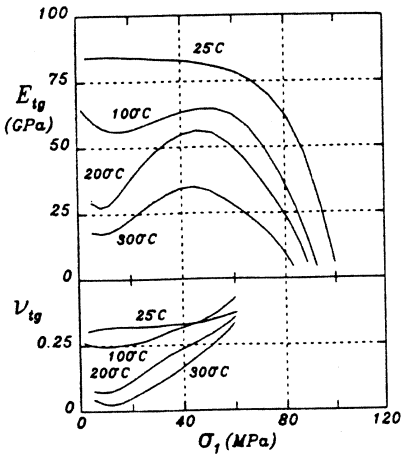

Figure 7. Tangent Young modulus and Poisson ratio as a function of stress for the specimens of fig.6

Fig.9 presents a comparison of the volumetric stress-strain curves obtained from isotropic triaxial compression tests carried out respectively on a specimen in natural conditions and on a specimen treated at 300°C. While the natural marble presents a linear and reversible behaviour, the curve relative to the microcracked material is sharply concave, and a considerable amount of the deformation is not recovered. Even at the maximum applied stress (60 MPa) the bulk modulus of the rock is markedly lower than that of undisturbed rock, and this proves that this stress is not sufficient to close all the microcracks.

5 DYNAMIC PROPERTIES

To investigate the dynamic characteristics of the rock, and the changes induced by the thermal treatment, compressional (V_P) and shear wave (V_S) velocities were determined in dry and saturated conditions by measuring the transit time of seismic pulses along the axis of an unstressed specimen (having the same geometry of those utilized for the uniaxial compression tests); coupling of the transducers to the ends of the specimens was assured by means of a slight load and by the application of a thin film of grease. The specimens were saturated by placing them in a vacuum vessel for 6 hours, after which deaerated water was introduced and the specimens were soaked for 24 hours.

The plot of seismic velocities versus total porosity (fig.10), shows that the P-wave velocity in dry specimens is very sensitive to microcracking.

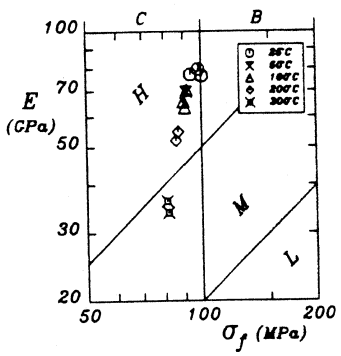

Figure 8. Deere-Miller diagram for natural and microcracked marble

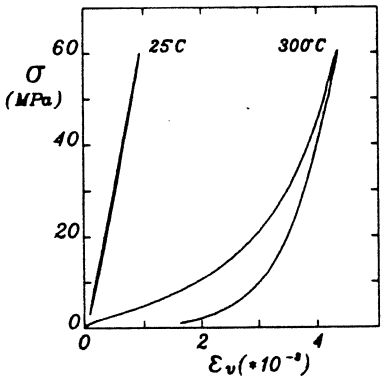

Figure 9. Volumetric strain curves of natural and 300°C specimens in isotropic triaxial compression tests

The difference ΔV_P between P-wave velocities for the same specimen in dry and saturated conditions (fig.11) is also a very efficient indicator of microcrack intensity; this parameter could be particularly useful in tests carried out in rocks for which the V_P value of the solid matrix is not exactly known. The same figure shows that the points representig the natural marble are very close to those of an ideal uncracked aggregate for which $\Delta V_P=0$; from the trend of the curve the theoretical velocity of this aggregate should be 6.5 km/s.

The effect of thermal cracking is also felt on the S-wave velocity, although the estimation of the transit time was, in this case, more uncertain and could not be made at all for the 300°C specimens in dry conditions. Saturation appears to affect also the shear wave velocity; this indicates that local equilibrium of water pressure between differently oriented cracks is not completely attained during wave propagation.

Compressional and shear wave velocities during uni-

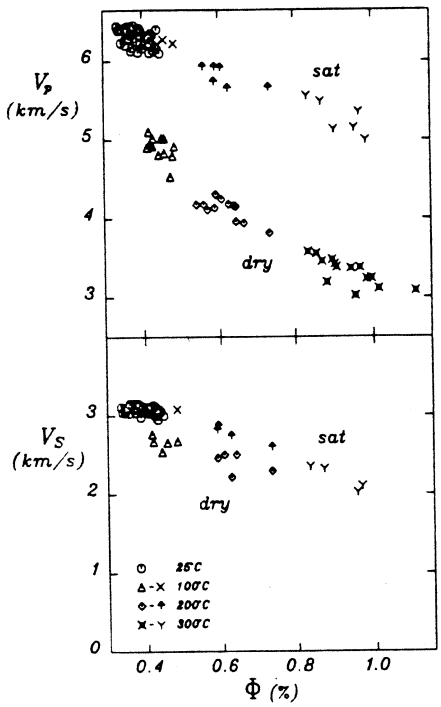

Figure 10. P- and S-wave velocities of natural and microcracked specimens in dry and saturated conditions as a function of total porosity

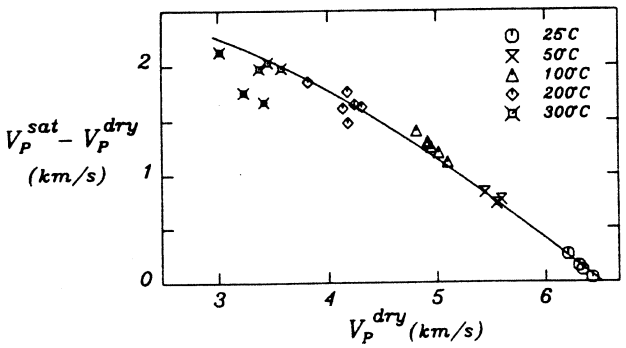

Figure 11. Difference between P-wave velocities in saturated and dry conditions for natural and microcracked specimens. The continuous curve indicates the analytical relationship according to the differential self-consistent method for isolated cracks, for an aspect ratio equal to $3 \cdot 10^{-3}$

axial and triaxial compression tests were also determined by means of the "Pundit" system (King, 1983), in which P- and S-wave broadband (300-800 kHz) transducers are mounted inside the platens of a conventional Hoek cell. A satisfactory acoustic coupling could be obtained at applied loads greater than 1-2 Mpa, without the need to interpose a thin load foil between the platens and the end faces of the specimen.

The plot of seismic velocities versus stress in the uniaxial compression test is shown in fig.12; unlike the trend of the corresponding stress-strain curves, the velocity of cracked rock increases steadily up to stress levels very near to peak strength. We also notice that the influence of the uniaxial stress is somewhat greater on the compressional than on the shear wave velocities. This behaviour is to be attributed to the fact that, when stress increases, the cracks with orientations that are nearly perpendicular to the applied load will close but, at the same time, axial cracks will be developing. The former factor tends to produce an increase in both V_P and V_S, whereas the second factor does not affect V_P but cause a decrease in V_S.

Finally, plots of seismic velocities in isotropic triaxial conditions are shown in fig.13; the velocities steadily increase with the applied pressure.

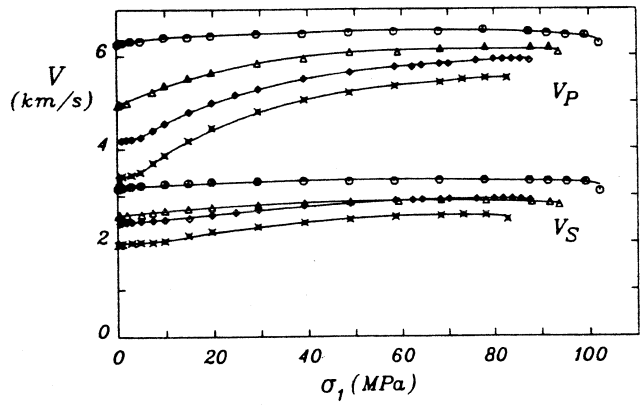

Figure 12. P- and S-wave velocities of natural and microcracked specimens vs applied stress in uniaxial compression tests. See fig.10 for symbols

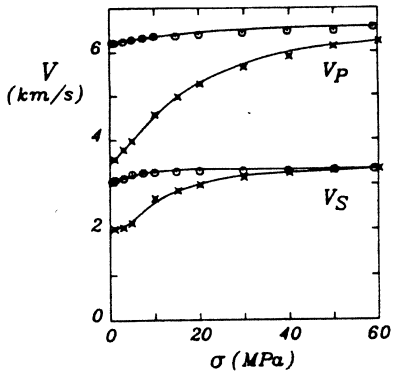

Figure 13. P- and S-wave velocities of natural and 300°C specimens as a function of applied stress in isotropic triaxial compression tests

6 ANALYSIS OF INDUCED MICROCRACKING

Most analytical theories for the mechanical behaviour of cracked solids in dry and saturated conditions are based on idealized models of the crack as thin oblate spheroids (penny-shaped cracks) (Kuster & Toksoz, 1974; O'Connell & Budiansky, 1974). These studies have shown that the elastic and dynamic characteristics of the cracked solids are not directly related to crack porosity but to the parameter (crack density) $e=N\langle a^3\rangle$, where N is the number of cracks per unit volume, and a is the radius of the cracks.

A differential self-consistent method (Cleary, 1978) is the best approach to evaluate the effect of crack density on elastic properties when the crack concentration is high; in the case of 300°C specimens e was found to be equal to 0.55. In this model compressional and shear wave velocities, in dry and saturated conditions, are related to each other. The experimental data for the V_P-V_S relationship show only partial agreement with the theoretical values (fig.14); a better agreement is observed for the values of V_P in dry and saturated conditions (fig.11).

The idealized model can also predict the applied stress at which closure of the cracks occurs as a function of the aspect ratio α, although this relationship is quite sensitive to slight departures from the model (Mavko & Nur, 1978). The variation of seismic velocities at increasing stress in triaxial isotropic tests could therefore be utilized to evaluate the distribution of both crack density and

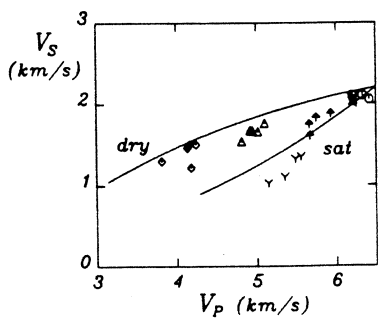

Figure 14. Correlation between P- and S-wave velocities of natural and microcracked specimens. The continuous curve indicates the analytical relationship according to the differential self-consistent method for isolated cracks, for an aspect ratio equal to $3 \cdot 10^{-3}$. See fig.10 for symbols

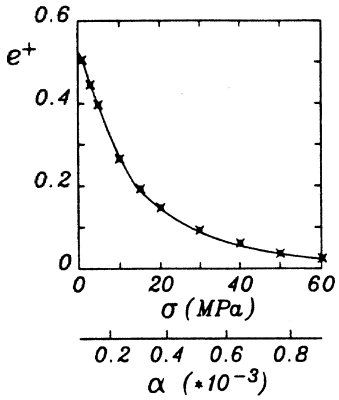

Figure 15. Density e^+ of open cracks as a function of the applied isotropic stress for a 300°C treated specimens; in the lower scale the aspect ratio of cracks closing at the stress σ

crack porosity as a function of closure pressure, which is related to α.

The results for the 300°C specimen, shown in fig.15, indicate that the large variation of seismic velocities in the range of isotropic loads of 0-60 MPa, should be due to cracks with an aspect ratio smaller than $1 \cdot 10^{-3}$. However, the corresponding variation of crack porosities estimated using the seismic data are not consistent with the strain values determined directly by means of extensometers, which are more than one order of magnitude greater. Apparently, the idealized crack model is not adequate to represent the behaviour of thermal microcracks; this is also confirmed by the large permanent deformations found in triaxial isotropic tests after unloading.

REFERENCES

BAUER, S.J. & B. JOHNSON 1979. Effects of slow uniform heating on the physical properties of the Westerly and Charcoal granites. 20th US Symp. Rock Mech., Austin.

BAUER, S.J. & J. HANDIN 1983. Thermal expansion and cracking of three confined, water-saturated igneous rocks to 800°C. Rock Mech. and Rock Eng. 16:181-198.

BRUNER, W.M. 1984. Crack growth during unroofing of crustal rocks: effects on thermoelastic behaviour and near-surface stresses. J. Geoph. Res. 89: 4167-4184.

CLEARY, M.P. 1978. Elastic and dynamic response regimes of fluid-impregnated solids with diverse microstructures. Int.J.Solids Structures 14:795-819.

EVANS, A.G. & D.R. CLARKE 1980. Residual stresses and microcracking induced by thermal contraction inhomogeneity. In Thermal Stresses in Severe Environments, p. 629-648. New York: Hasselman & Heller.

FREDRICH, J.T. & T.-F. WONG 1986. Micromechanics of thermally induced cracking in three crustal rocks. J. Geoph. Res. 91: 12743-12764.

GEROGIANNOPOULOS, N.G. & E.T. BROWN 1978. The critical state concept applied to rock. Int. J. Rock Mech. Min. Sci. 15: 1-10.

HOMAND-ETIENNE, F. & R. HOUPERT 1989. Thermally induced microcracking in granites: characterization and analysis. Int.J.Rock Mech. Min. Sci. 26:125-134.

JOHNSON, B., A.F. GANGI & J. HANDIN 1978. Thermal cracking of rock subjected to slow, uniform temperature changes. 19th US Symp. Rock Mech., Nevada: 259-267.

KAWAMOTO, T., Y. ICHIKAWA & T. KYOYA 1988. Deformation and fracturing of discontinuous rock mass and damage mechanics theory. Int. J. Num. Anal. Method Geomech. 12: 1-30.

KING M.S. 1983. Static and dynamic elastic properties of rocks from the Canadian Shield. Int. J. Rock Mech. Min. Sci. & Geomech. Abstr. 20: 237-241.

KUSTER, G.T. & N.M. TOKSOZ 1974. Velocity and attenuation of seismic waves in two-phase media: Part I. Theoretical formulations. Part II. Experimental results. Geophysics 39: 587-618.

MAVKO, G.M. & A. NUR 1978. The effect of nonelliptical cracks on the compressibility of rocks. J. Geoph. Res. 83: 4460-4468.

NUR, A. & G. SIMMONS 1970. The origin of small cracks in igneous rocks. Int. J. Rock Mech. Min. Sci. 7: 307-314.

O'CONNELL, R.J. & B. BUDIANSKY 1974. Seismic velocities in dry and saturated cracked solids. J. Geoph. Res. 79: 5412-5426.

PERAMI, R. 1971. Formation des microfissures dans les roches sous l'effet de variations homogènes de température. Int. Symp. ISRM Fissuration des Roches, Nancy.

ROSENGREN, K.J. & J.C. JAEGER 1968. The mechanical properties of an interlocked low-porosity aggregate. Geotechnique 18: 317-326.

SIMMONS, G. & H. WANG 1971. Single crystal constants and calculated aggregate properties: A Handbook. Cambridge: MIT Press.

SIMMONS, G. & H.W. COOPER 1978. Thermal cycling cracks in three igneous rocks. Int. J. Rock Mech. Min. Sci. 15: 145-148.

SKINNER, B.J. 1966. Thermal expansion. In Handbook of physical constants. The Geological Society of America Memoir 97.

THILL, R.E., J.R. McWILLIAMS & T.R. BUR 1968. An acoustical bench for an ultrasonic pulse system. Bureau of Mines: 1-22.

Research supported by a M.P.I. grant (40%)